ARTICLE

Evaluation of the thermal stability under air of the uranyl peroxide nanocluster $(NH_4)_{40}[(UO_2)_{32}(O_2)_{40}(OH)_{24}]\cdot nH_2O$

Paul-Henri Imbert[a], Olivier Tougait[a*], Philippe Devaux[a], Natacha Henry[a], Marine Ellart[a], Francis Abraham[a] and Jérémy Nos[b]

[a]*Univ Lille, UCCS - UMR CNRS 8181, ENSCL-USTL, BP 90108, 59652 Villeneuve d'Ascq Cedex, France;* [b]*AREVA-NC,Tour AREVA, 1 Place Jean Millier, 92084 Paris La Défense, France*

The synthesis, characterization and thermal decomposition of the uranyl peroxide nanocluster $(NH_4)_{40}[(UO_2)_{32}(O_2)_{40}(OH)_{24}].nH_2O$, designated as U32R-NH$_4$, are presented for a series of temperatures ranging from 20 to 800°C. The handlings and annealing were carried out under air and the post-treatment characterizations were managed back to room temperature. The identification of the intermediate compounds was achieved by chemical analysis, infrared spectroscopy and powder X-ray diffraction. The proposed decomposition scheme up to U_3O_8 comprises three main steps; (*i*) the low temperature range, from room temperature to 190°C, is characterized by the loss of the molecular species, water molecules, ammonium and peroxo ions, (*ii*) the intermediate temperature range, from 190 to 590°C, involves mostly structural rearrangements and release of oxygen and nitrogen species, and (*iii*) the high temperature range, above 590°C, which is associated to the $UO_3 - U_3O_8$ transition accompanied with O_2 release. The thermal treatment up to 800°C does not alter the morphological features of the initial powder suggesting a pseudomorphic decomposition. Upon ageing or heating, the starting compound, $(NH_4)_{40}[(UO_2)_{32}(O_2)_{40}(OH)_{24}].nH_2O$, readily loses its crystallinity.

Keywords: thermal decomposition; chemical analysis; infrared spectrum; powder X-ray diffraction; uranium oxide; pseudomorphic decomposition

1. Introduction

Mixed U^{6+}/Pu^{4+} solid compounds precipitated from aqueous solutions are regarded as possible precursors for MOX fabrication [1]. To this respect, the recent advances on the synthesis and structural characterization of uranyl peroxide nanoclusters containing rare-earth cations [2] afford the opportunity of an innovative fabrication process, interesting to explore. This family of compounds is characterized by a framework built from uranyl polyhedra bridged through peroxide or hydroxide ligands [3,4] that create cavities where the countercations reside. Their high structural and chemical flexibilities yielding assemblies described as nanoclusters, afford about 40 original arrangements reported in the literature.

Among them, the uranyl peroxide, $(NH_4)_{40}[(UO_2)_{32}(O_2)_{40}(OH)_{24}]\cdot nH_2O$, denoted in the following as U32R-NH$_4$, readily precipitates at room temperature with a sharp selectivity [5]. Its high anionic moiety associated to its crown shape make it rather promising for intercalation chemistry. Very recently we successfully exchanged the NH_4^+ by Nd^{3+} or Th^{4+}

cations [6], allowing prospective research for the fabrication of mixed fuel or target, combining uranium and trans-uranium elements by considering Th^{4+} and Nd^{3+} as a surrogate of Pu^{4+} and Am^{3+}, respectively. The scientific objective of our study is to demonstrate the potentiality of these nanoclusters as suitable precursors for the preparation of single phase fluorine type mixed oxides pellets, with optimized microstructure.

As a first step of this exhaustive study, we present here the investigation on the stability behaviors of the nano-uranyl cluster U32R-NH$_4$. The thermal decomposition pathway was studied by *ex-situ* annealing at key temperatures by means of chemical analysis, infrared spectroscopy and powder X-ray diffraction on the intermediate reaction products.

2. Experimental section

2.1. U32R-NH$_4$ synthesis

The ammonium uranyl peroxide nanocluster $(NH_4)_{40}[(UO_2)_{32}(O_2)_{40},(OH)_{24}]\cdot nH_2O$, denoted as U32R-NH$_4$, was synthesized by adding a solution of uranyl nitrate hexahydrate $(UO_2(NO_3)_2\cdot 6H_2O$, 0.34 M) and hydrogen peroxide (H_2O_2, 9.79 M). Under

---

*Corresponding author. Email: olivier.tougait@univ-lille1.fr

continuous stirring, a solution of ammonium hydroxide (NH_4OH, 4 M) was added until the pH reaches 10. After precipitation and ageing time at room temperature of about 10 hours, the solid was filtered under vacuum and washed with 5 ml of ethanol. Finally, the powder was dried at room temperature.

2.2. Heat treatment

Annealing of batches of powders was carried out for 16 hours under air with a heating ramp of 5°Cmin^{-1} up to the target temperature. For temperatures up to 200°C, the calcinations were performed in computer controlled ovens whereas for temperatures above 200°C, they were performed in resistance furnaces.

2.3. Scanning electron microscopy (SEM)

Scanning Electron Microscopy (SEM) was carried out with a Hitachi S4700 SEM FEG microscope.

2.4. Thermogravimetric (TGA) and differential thermal analyses (DTA)

Thermogravimetric and differential thermal analyses were carried out with a SETARAM 92 system. The sample was placed in an alumina crucible and heated up to 800 °C, in air, with a scan rate of 5°Cmin^{-1}.

2.5. Chemical analyses

The inductively coupled plasma atomic emission spectroscopy (ICP-AES) analysis of U was conducted using a VARIAN Vista-Pro instrument. About 10 mg of powder was dissolved in nitric acid (HNO_3, 8M). Subsequent dilutions were carried out to reach a uranyl ion concentration in the range 20 to 40 ppm.

The weight percentage of ammonium ions was determined by a metric pH assay (Kjeldahl method). The kjeldahl distiller used is the Kjelflex-360. The automatic titrator is Titroline 5000. The weight percentage of peroxide ions was determined by redox titration.

2.6. Spectroscopic measurement

Infrared spectra were measured on PerkinElmer Spectrum Two spectrometer between 4000 and 400 cm^{-1}, equipped with a diamond attenuated total reflectance (ATR) accessory.

2.7. Powder X-ray diffraction (XRD) analysis

Room temperature XRD diagrams were collected with a D8 Advance Bruker diffractometer (Ө-Ө mode, CuKα radiation) equipped with a Vantec1 linear position sensitive detector (PSD). Each diagram was recorded in the range 5-60° (2Ө), with a step of 0.02° and with a speed of 0.5 s/step.

3. Results and discussion

Figure 1 shows the thermal decomposition under air of the compound U32R-NH_4. The thermogravimetric

curve and its derivative reveal three significant weight losses as outlined by the calculated weigh percent of the intermediate compositions. The first decomposition step occurs below about 190°C for a mass loss of 17 wt %. The second one, which is characterized by a continuous weight loss of 6% and a featureless derivative extends up to about 590°C. The last decomposition step takes place at 590°C with a 3.5 wt% loss.

The differential thermal analysis (DTA) curve indicates a more tangled scheme associated to five distinct thermal effects. The first decomposition step, below about 190°C is characterized by two thermal accidents, at 70°C and about 150°C, coupled to endodermic and exothermic peaks respectively. The second decomposition step ranges from 190 to 590°C and exhibits three successive exothermic peaks with onset temperature at about 220°C, 280°C and 380°C. The third decomposition step occurs as a single transition at about 590°C. This last endotherm can be readily associated to the transformation of UO_3 to U_3O_8.
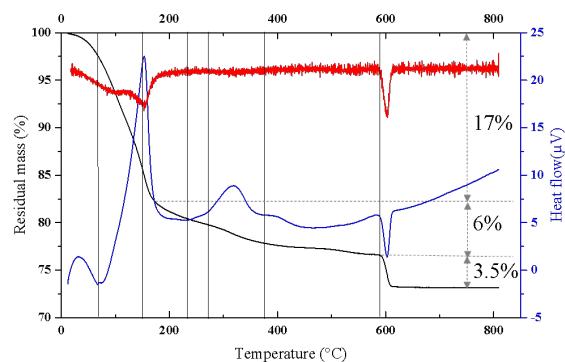

Figure 1.   Decomposition of U32R-NH_4 in air: TG trace is the black curve and its derivative is the red curve; DTA signal is in blue. Vertical thin lines point out the main transformations.

Ex-situ annealing temperatures were chosen below and above each thermal accident, roughly corresponding to shallow plateaus of the TGA curve. They were determined as 70°C, 200°C, 350°C, 470°C, 570°C and 800°C. The heat-treated samples were used to identify and to characterize the intermediate phases of the thermal decomposition of U32R-NH_4 peroxide in order to support a stepwise scheme.

Figure 2 shows the samples retrieved after each annealing. The evolution of the color follow the typical trend of yellow, orange, red, brown, green and black which is associated to the reduction from U^{6+} to U^{4+} of uranium ions and their contents in solids.

Figure 2.   Samples retrieved from stepwise annealing, of the intermediate reaction powders of U32R-NH_4.

Figure 3 displays SEM images of each heat-treated powder which more likely appears as aggregates of submicronic particles and micrometric single crystals with elongated rice seed shape. The samples description

remains the same for all the annealed powder indicating that thermal treatment does not alter the powder morphology in agreement with a possible pseudomorphic decomposition of the U32R-NH₄ material.
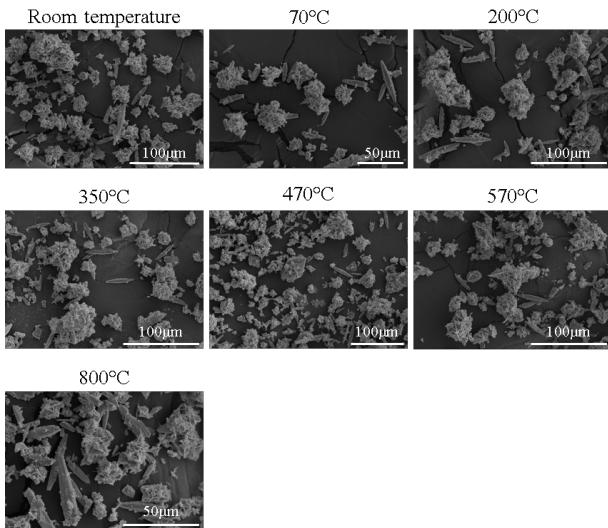

Figure 3. SEM images, collected in secondary electron mode, of intermediate reaction powders of U32R-NH₄ produced by heating treatment at selected temperatures for 16 hours.

The IR spectra of U32R-NH₄ and the products obtained by heating the solid at 70, 200, 350, 470, 570 and 800°C and cooling to room temperature are gathered in **Figure 4**. In agreement with the crystalline structure, $(NH_4)_{40}[(UO_2)_{32}(O_2)_{40}(OH)_{24}] \cdot nH_2O$, the IR spectra indicate absorption bands featuring the three main constitutional groups, NH_4^+, UO_2^{2+} and H_2O. The room temperature spectrum exhibits a broad band ranging from 3600 to 2700 cm^{-1} which may be assigned to the various stretching modes of H_2O and NH_4^+, whereas the shaper absorption bands in the range 1650-1200 cm^{-1} may be associated to the bending modes of these molecules. The strong peak in the neighborhood of 900 cm^{-1} along with its shoulder at about 850 cm^{-1} are undoubtedly due to the symmetric and asymmetric vibrations of the uranyl ion [7]. Absorption bands featuring the vibrational stretching modes of the peroxo ion and the $UO_2^{2+} - O_2^{2-}$ linkage could not be detected. The IR spectra of the stepwise annealed samples were used as footprint of the release of the H_2O and NH_3 molecules and the structural evolution of the UO_2^{2+} geometry. The vanishing of the absorption bands in the range 3600-2700 cm^{-1} indicates that the loss of the H_2O and NH_4^+ arises below 200°C. The weak but apparent absorption bands between 1650-1200 cm^{-1} in the 200°C spectrum may be ascribed to the U–OH and U–NH bending vibrations [8]. Starting from 200°C, a clear evolution of the U-O vibration modes arises, outlined by the lowering of the 900-850 cm^{-1} narrow bands and the growing of the 860-600 cm^{-1} thick bands. It results from the elongation of the (U=O$_{yl}$) distances and angles toward a (U–O) bonds of typical coordination polyhedron [8].
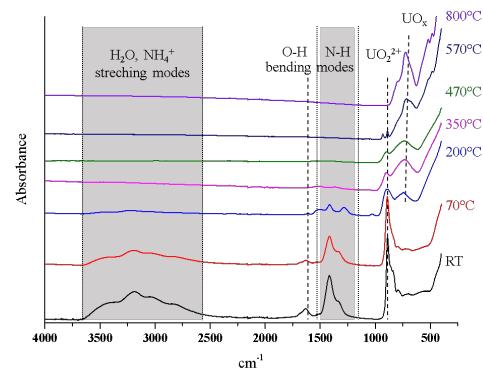

Figure 4. IR spectra of samples from stepwise annealing at the key temperatures of intermediate reaction phases of U32R-NH₄.

Figure 5 shows the powder X-ray patterns of the stepwise samples annealed under air. Absence of diffracted intensity in patterns from room temperature to 470°C indicates amorphous phases emphasizing the loss of the U32R-NH₄ crystallinity after ageing for 10h.
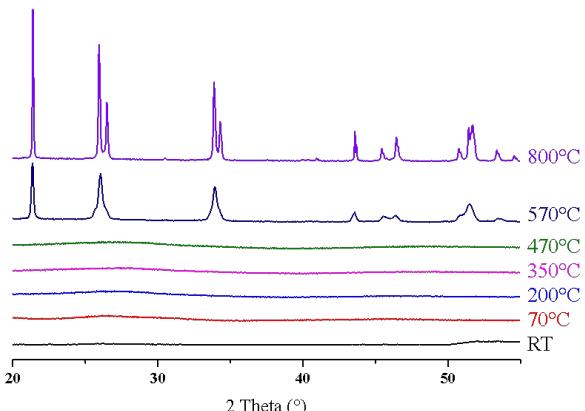

Figure 5. Powder X-ray diffraction patterns of samples retrieved from different temperatures.

The diffraction pattern of the 570°C heat-treated sample collected back to room temperature was indexed by considering a mixture of two oxide phases, (*i*) αUO₃ with its commonly accepted average description in hexagonal symmetry [9] and (*ii*) UO$_{2.9}$ having an orthorhombic symmetry [10] with the refined parameters a = 6.912(1) Å, b = 3.910(1) Å, c = 4.153(1) Å. The 800°C pattern was fully indexed with the αU₃O₈ in the *C2mm* orthorhombic space group, in agreement with [11].

The results of the chemical analyses of the annealed samples are presented in Table 1. They clearly show the vanishing of the peroxo ions below 200°C and the continuous decrease of the ammonium ions up to 350°C.

4. Conclusion

Results of thermal decomposition studies of the solid are summarized in **Table 1**. The correlation of the chemical, infrared and powder X-ray diffraction

Table 1.   Summary of the results of chemical, infrared, powder-XRD analyses for the key temperatures.

Temperature	Identification of active species in Infrared	Crystalline phases XRD	Chemical (% weight)	Proposed phases
RT	NH_4^+ , H_2O, N-H, O-H, UO_2^{2+}		$NH_4^+ = 5.1$ $O_2^{2-} = 7.5$	$(NH_4)_{40}[((UO_2)_{32}(O_2)_{40}(OH)_{24})]\cdot nH_2O$
70°C	NH_4^+ , H_2O N-H, O-H, UO_2^{2+}	amorphous	$NH_4^+ = 3.9$ $O_2^{2-} = 5.8$	amorphous $(NH_4)UO_3$ $amUO_3$
200°C	O-H, N-H UO_2^{2+}, U-O		$NH_4^+ = 1.3$ $O_2^{2-} = 0.1$	
350°C	N-H U-O		$NH_4^+ = 0.5$	
470°C	U-O			
570°C	U-O	$\alpha UO_3 + UO_{2.9}$		$\alpha UO_3 + UO_{2.9}$
800°C	U-O	αU_3O_8		αU_3O_8

analyses of annealed samples at key temperatures in support of the thermal analysis allows to propose the thermal decomposition scheme of U32R-NH4. The TGA curve shows a substantial weight loss up to 190°C, corresponding to the loss of water, ammonium and peroxo species. Upon heating to 590°C, the TGA curve displays three small weight losses which may be ascribed to the release of elemental N or O species (NH+ or OH+) that are structurally bonded to U atoms. The structural rearrangement is in line with the three exothermic peaks observed in DTA curve. At 590°C, UO_3 undergoes transformation to U_3O_8 which is associated to an endothermic peak. A total mass loss of 26.5 % is observed experimentally during thermal decomposition, which is in agreement with the calculated one of 25.5 % from $(NH_4)_{40}[(UO_2)_{32}(O_2)_{40}(OH)_{24}]\cdot nH_2O$ (with n = 56) to U_3O_8.

The indexation of the X-ray pattern of the sample annealed at 570°C with two uranium trioxide phases violates the Gibbs rule for a binary system, at a given partial oxygen pressure. It suggests a possible re-oxidation of the 570°C stable phase upon cooling in air [12] or the presence of light molecules stabilizing one of these crystalline forms [13]. In order to study the thermal decomposition of U32R-NH4, *in-situ* analyses are required.

References
[1] F. Abraham, B. Arab-Chapelet, M. Rivenet, C. Tamain and S. Grandjean, Actinide oxalates, solid state structures and applications, *Coord. Chem. Rev.* 266-267 (2014), pp.28-68.

[2] F. Blanchard, F. Abraham, M. Rivenet, S. Grandjean, N. Vigier and I. Hablot, Patent FR3015453, WO2015091753, (2015).

[3] J. Qiu and P.C. Burns, Clusters of actinides with oxide, peroxide, or hydroxide bridges, *Chem. Rev.* 113 (2013), pp. 1097-1120.

[4] F. Blanchard, M. Ellart, M. Rivenet, N. Vigier, I. Hablot, B. Morel, S. Grandjean and F. Abraham, Role of ammonium ions in the formation of ammonium uranyl peroxides and uranyl peroxo-oxalates, *Cryst. Growth Des.* 16 (2016), pp. 200-209.

[5] G.E. Sigmon and P.C. Burns, Rapid self-assembly of uranyl polyhedra into crown clusters, *J. Am. Chem. Soc.* 133 (2011), pp.9137-9139.

[6] F. Blanchard, M. Ellart, M. Rivenet, N. Vigier, I. Hablot, B. Morel, S. Grandjean and F. Abraham, Neodymium uranyl peroxide synthesis by ion exchange on ammonium uranyl peroxide nanoclusters, *Chem. Comm.* 52 (2016), pp.3947-3950.

[7] N.H. Rofail, Infrared and x-ray diffraction spectra of ammonium uranyl carbonate, *Mater. Chem. Phys.* 36 (1994), pp. 241-245.

[8] R.L. Frost, J. Čejka, G.A. Ayoko and M.L. Weier, Vibrational spectroscopic study of hydrated uranyl oxide: Curite, *Polyhedron* 26 (2007), pp. 3724-3730.

[9] W.H. Zachariasen, Crystal chemical studies of the 5f-Series of elements. I. New structure types, *Acta Crystallogr.* 1 (1948), pp. 265-268.

[10] H.R. Hoekstra and S. Siegel, The uranium-oxygen system: U3O8-UO3, *J. Inorg. Nucl. Chem.* 18 (1961), pp. 154-165.

[11] B.O. Loopstra, Neutron diffraction investigation of U3O8, *Acta Crystallogr.* 17 (1964), pp 651-654.

[12] B.O. Loopstra, The Phase transition in α-U308 at 210°C, *J. Appl. Cryst.* 3 (1970), pp. 94- 95.

[13] H.R. Hoekstra and S. Siegel, The uranium trioxide-water system, *J. Inorg. Nucl. Chem.* 35 (1973), pp. 761-779.